J. Chem. Sci., Vol. 122, No. 4, July 2010, pp. 471–480.

Study of multi-site chemical exchange in solution state by NMR: 1D experiments with multiply selective excitation

SAMANWITA PAL

Department of Chemistry, Indian Institute of Technology – Madras, Chennai 600 036
e-mail: samanwitapal@gmail.com

MS received 14 January 2010; revised 21 April 2010; accepted 27 May 2010

Abstract. Chemical exchange in solution state has been investigated traditionally by both 1D and 2D NMR, permitting the extraction of kinetic parameters (e.g. the spin-lattice relaxation time T_1, the exchange rate constant k and the activation parameters). This work demonstrates a simple 1D NMR approach employing multiply selective excitation to study multi-site exchange processes in solution, applying it to systems that exhibit three-site exchange. This approach involves simultaneous excitation of all – or a chosen subset of – the exchanging sites by using an appropriately modulated shaped radiofrequency pulse. The pulse sequence, as well as analysis is summarized. Significant features of the experiment, which relies on sign labelling of the exchanging sites, include considerably shorter experiment time compared to standard 2D exchange work, clear definition of the exchange time window and uniform pulse non-ideality effects for all the exchanging sites. Complete kinetic information is reported in the study of dynamic processes in superacid solutions of two weak bases, studied by ^{1}H NMR. An analytical solution, leading to the determination of four rate parameters, is presented for proton exchange studies on these systems, which involve a mixture of two weak bases in arbitrary concentration ratio, and stoichiometric excess of the superacid.

Keywords. Chemical exchange; solution state; 1D NMR; modulated shaped RF pulses; multi-site selection; sign labelling.

1. Introduction

Chemical exchange in solution state has been investigated over the years by both 1D and 2D NMR methods.[1–17] In general, one-dimensional (1D) magnetization transfer (MT) experiments[9,18–31] or T_1-based experiments offer better prospects for quantitation of the exchange processes compared to lineshape analysis methods[1,2,16] which are T_2-based experiments. In the slow exchange regime the two-dimensional (2D) exchange experiment[12] is an excellent tool to investigate the exchange process both qualitatively and quantitatively. Each of these methods has its own merits and demerits. Although 2D EXSY is unrivaled in probing chemical exchange, the time required for complete quantitation by standard EXSY[12] is a major issue. More recently, an ultrafast 2D exchange experiment[32] has been proposed, that permits the acquisition of a complete set of mixing incremented 2D exchange patterns within a single experiment entailing a total time of *ca*. 1 s. 1D MT experiments on the other hand do not throw light on the exchange pathways and need prior knowledge of the chemical shifts of the exchanging sites.

The present work proposes an efficient 1D method to study multi-site exchange processes in solution[33–35] by NMR, and illustrate the current approach with studies on a system that exhibits three-site exchange.[36, 37] The pulse sequence is given in figure 1 along with the standard 2D EXSY sequence for comparison. This approach involves simultaneous excitation of all – or a chosen subset of – the exchanging sites by using an appropriately amplitude modulated shaped ($\pi/2$) pulse at the beginning of the sequence which is immediately followed by a hard ($\pi/2$) pulse. Together, these two pulses result in selective rotation of magnetization of a chosen set of sites by a desired angle, e.g. 0° or 180°. Thus, the z-magnetization of the spins is sign labelled, being placed in the $\pm z$ direction at the start of the mixing time, depending on the kind of modulation used for the first pulse, and permitting thereby the creation of various initial states. During the

exchange period (τ_m), longitudinal magnetization is subject to spin-lattice relaxation as well as exchange. The last hard $\pi/2$ pulse brings the magnetization back to the transverse plane for detection. By varying τ_m one may monitor the return of magnetization to equilibrium. In keeping with the way the sequence functions, it is termed as the 'multi-site selective inversion experiment'. Significant features include considerably shorter experiment time compared to standard 2D EXSY,[12] clear definition of the exchange time window, and uniform pulse non-ideality effects for all the exchanging sites.

Double modulation of the shaped pulse envelope has been employed to investigate three site exchange. Table 1 sets out the phase cycle that have been implemented for the double cos and double sin modulated inversion experiments, as well as that for the cos–sin and sin–cos modulated inversion experiments; the purpose of the phase cycle is the suppression of signal components that arise from pulse imperfections.

2. Experimental

Multi-site selective inversion experiments were carried out at a series of temperatures and at a number of τ_m values on a Bruker Avance 400 NMR spectrometer with a 5·4 cm vertical bore magnet, employing a Bruker 5 mm BBO probehead. The Bruker variable temperature unit BVT-3200 was used to measure and regulate the temperature during the experiments.

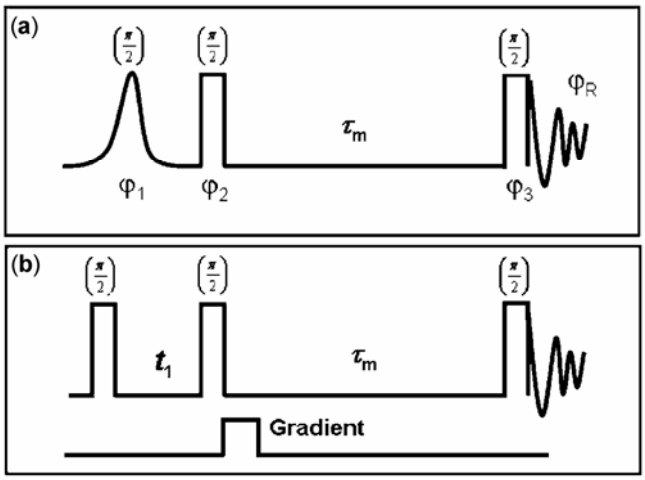

Figure 1. (**a**) The 1D exchange pulse sequence involving modulated shaped pulse, φ: phase of the pulses and the receiver; the phase cycle is given separately in a tabular form, (**b**) the 2D exchange pulse sequence involving three hard pulses. The rectangular bars denote $\pi/2$ pulses whereas the non-rectangular shape denotes the modulated shaped pulse.

Modulated shaped pulses were generated using the Bruker 'shapetool', invoking the appropriate modulation frequencies. A Gaussian envelope[38] has been used as the basic shape, whose amplitude is doubly modulated with cosine and/or sine wave(s) to produce four excitation sidebands respectively. The shaped pulse duration has been set to be shorter than the anticipated exchange lifetime; the pulse duration used in the present study is 10 ms.

2.1 *Shaped pulse modulation*

To achieve tri-selective excitation, the transmitter frequency (ν_T) may be positioned at the average of any two of the three chemical shifts in question, denoted by ν_A, ν_B, ν_C, here, ν_A corresponds to the lowest frequency signal, the next higher frequency signal being at ν_B the highest frequency line being at ν_C. The two modulation frequencies (ν_{m_1}, ν_{m_2}) are then given as half the modulus of the difference in frequencies between the third line and each of the chosen two lines in turn. The redundant frequency generated is given by the sum of the frequencies of the two chosen lines, minus that of the third. As an example, if the transmitter be placed at the mean frequency of the two highest frequency lines, ν_B and ν_C (i.e. $\nu_T = (\nu_B + \nu_C)/2$), the two modulation frequencies are given by: $\nu_m = (\nu_B - \nu_A)/2$ and $\nu_m = (\nu_C - \nu_A)/2$. The redundant frequency is in turn given by $\nu_R = \nu_B + \nu_C - \nu_A$.

Four different double modulation schemes of the shaped pulse are possible, viz. double cosine, cosine–sine, sine-cosine and double sine, in keeping with a Hadamard matrix[39] of order 4. Simple trigonometric relations may be used to find the outcome of such double modulation schemes. Table 2 summarizes the phase relations among the four excitation frequencies for the four modulation schemes, the carrier being placed at the average of the two highest frequency peaks (ν_B, ν_C).

2.2 *Materials*

An equimolar mixture of fluorosulphonic acid (FSO_3H) and antimony pentafluoride (SbF_5), (known as 'magic acid'[40,41]) was procured from Sigma-Aldrich and used as the solvent acid (site 1) without further purification or drying. To 0·41 ml of

Table 1. Phase cycle used for the double modulated multi-selective inversion recovery experiment.

Modulation employed*	Scan	φ_1	φ_2	φ_3	φ_R
Double cosine	1	0	0	0	0
	2	2	2	0	0
Cosine–sine	1	3	0	0	0
	2	1	2	0	0

*The first descriptor designates the modulation frequency ν_{m_1}, while the second designates ν_{m_2}

Table 2. Excitation phase relations obtained for four double modulation schemes with the transmitter being placed at the average of ν_B and ν_C.

	Relative phase of the chemical sites excited			
Modulation employed*	$\nu_{\text{fictitious}}$	ν_C	ν_B	ν_A
cos–cos	+	+	+	+
cos–sin	+	+	–	–
sin–cos	+	–	+	–
sin–sin	+	–	–	+

*The first descriptor designates the modulation frequency ν_{m_1}, while the second designates ν_{m_2}

the solvent acid (HA), 0·01 ml of water (the first solute base, B) and 0·055 ml of acetone (the second solute base, C), were added directly. Water and acetone are fully protonated under this condition. The conjugate acids of the solute bases B and C, viz. HB^+ and HC^+ denote site 2 and site 3 respectively. The sample therefore contains exchangeable protons in three different sites with the equilibrium population ratio $HA : HB^+ : HC^+ = 5 : 1 : 1$, as determined from the NMR spectral intensities. The dynamics of proton exchange observed in the superacid solution may be modelled as a three-site exchange process.

3. Analysis

Analytical solutions of the relevant kinetic equations, formulated using the modified Bloch-McConnell equations[42] are available in the literature[43] for both two-site and equally populated three-site exchange processes.

The kinetic equations for a closed three-site exchange network[44] involving three unequally populated sites do not in general have an analytical solution for arbitrary initial conditions, since a total of nine unknown rate parameters, viz. three different pairs of pseudo-first order rate constants (one pair between each pair of exchanging sites, viz. k_{12}, k_{21}, k_{13}, k_{31}, etc.), as well as three different spin-lattice relaxation rates (one corresponding to each site) have to be considered. Hence numerical solutions[33,45] are preferred in the general context. However, analytical solutions to determine all the nine parameters of a general three-site exchange process are available in the literature, considering extensive combinations of saturation transfer and inversion recovery experiments.[46,47]

In the case of proton exchange dynamics in superacid media,[36,37] a closed exchange network as given in figure 2 has been considered. A 2D EXSY spectrum of the superacid solution at $T = 298$ K, given in figure 3, confirms this. The corresponding Bloch-McConnell equations for such a general three site exchange process involving three unequally populated sites exchanging among each other may be written as follows:

$$\frac{\mathrm{d}I_z}{\mathrm{d}t} = \left[-\frac{(I_z - I_0)}{T_{11}} - \left(k_{12} + k_{13}\right) I_z + k_{21} S_z + k_{31} R_z \right], \tag{1}$$

$$\frac{\mathrm{d}S_z}{\mathrm{d}t} = \left[-\frac{(S_z - S_0)}{T_{12}} - (k_{21} + k_{23}) S_z + k_{12} I_z + k_{32} R_z \right], \tag{2}$$

$$\frac{dR_z}{dt} = \left[-\frac{(R_z - R_0)}{T_{13}} - (k_{31} + k_{32})R_z + k_{23}S_z + k_{13}I_z \right]. \quad (3)$$

Here I_z, S_z, R_z I_z, S_z, R_x are z-magnetizations at any time t at sites 1, 2, 3 respectively, while I_0, S_0, R_0 represent the corresponding equilibrium magnetizations. T_{1i} represents the spin-lattice relaxation time of site i and k_{ij} is the rate constant for the exchange of magnetization from site i to site j.

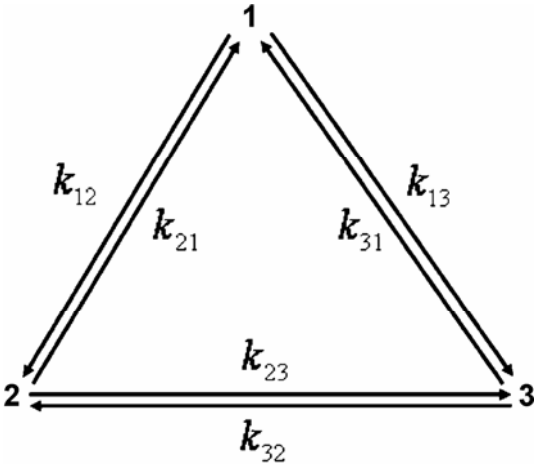

Figure 2. The three-site exchange network. Exchange is going on simultaneously among all the three sites denoted as 1, 2 and 3.

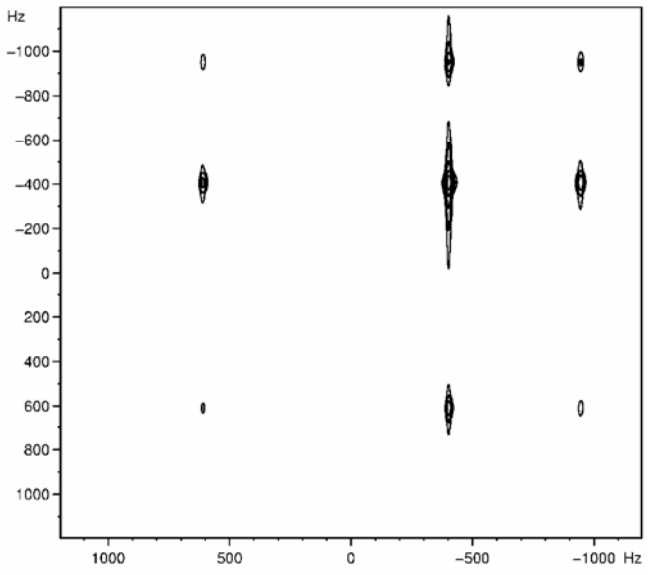

Figure 3. 2D EXSY spectrum of superacid solution containing water and acetone as the solute bases. The spectrum is acquired with a mixing time of 350 ms at T = 298 K. The spectrum was recorded with 2 K t_2 points and 128 t_1 points and D1 + AQ = 7 s for a spectral width of 2·4 kHz. 16 scans were acquired per t_1 increment.

By invoking microscopic reversibility at dynamic equilibrium[48] the above set of coupled inhomogeneous differential equations may be readily cast in homogeneous form, corresponding to the matrix given in (4).

$$\frac{d}{dt}\begin{pmatrix} I_z - I_0 \\ S_z - S_0 \\ R_z - R_0 \end{pmatrix} = \begin{pmatrix} \begin{pmatrix} -\frac{1}{T_{11}} - k_{12} \\ -k_{13} \end{pmatrix} & k_{21} & k_{31} \\ k_{12} & \begin{pmatrix} -\frac{1}{T_{12}} - k_{21} \\ -k_{23} \end{pmatrix} & k_{32} \\ k_{13} & k_{23} & \begin{pmatrix} -\frac{1}{T_{13}} - k_{32} \\ -k_{31} \end{pmatrix} \end{pmatrix} \begin{pmatrix} I_z - I_0 \\ S_z - S_0 \\ R_z - R_0 \end{pmatrix}. \quad (4)$$

In the present case the Bloch–McConnell equations have been formulated taking into account the following considerations:

(i) Within experimental error the system exhibits a single spin-lattice relaxation time, i.e. $T_{1i} = T_1$; i = 1, 2, 3, over the temperature range from 25°C to –40°C.

(ii) Concentration of the superacid (HA) is very high compared to the solute bases (B, C). Under these conditions, complete protonation of the two solute bases is guaranteed.

Subject to these two conditions, analytical solutions of the kinetic matrix may be found for any arbitrary initial conditions using Mathematica, employing the actual population ratio of the three components. In the present study, the equilibrium populations are in the ratio $p_1 : p_2 : p_3 = 5 : 1 : 1$, p_i denoting the equilibrium population of the ith site as measured from the NMR intensities. Invoking microscopic reversibility at dynamic equilibrium[48]

the following relations may be written considering the population ratios mentioned:

$$k_{12} = 0{\cdot}2k_{21}; \quad k_{13} = 0{\cdot}2k_{31}; \quad k_{23} = k_{32}. \tag{5}$$

Further, following the arguments of Gold *et al*[37] and using the second constraint of excess superacid concentration, one eventually arrives at a single experimental first order rate constant for the two exchange processes: between sites 1, 2 (k_{12}) as well as between sites 1, 3 (k_{13}). Under these conditions, in fact, the resulting kinetic equation matrix has only three unknown parameters, viz. the single spin-lattice relaxation time and two different experimental first order rate constants. This may be further appreciated on considering the following points.

The system under investigation contains three individual equilibrium processes going on simultaneously. One is given by:

$$HA + B \underset{k_{HB,A}}{\overset{k_{HA,B}}{\rightleftharpoons}} HB^{+} + A^{-}. \tag{6}$$

Here the second order rates, viz. $k_{HA,B}$ and $k_{HB,A}$ are related to the corresponding first order rate constants[37] as given below:

$$k_{HA,B} = \frac{k_{12}}{[B]}, \tag{7a}$$

$$k_{HB,A} = \frac{k_{21}}{[A^{-}]}. \tag{7b}$$

The other two equilibrium processes along with the respective second order rates are given below:

$$HA + C \underset{k_{HC,A}}{\overset{k_{HA,C}}{\rightleftharpoons}} HC^{+} + A^{-}. \tag{8}$$

Here

$$k_{HA,C} = \frac{k_{13}}{[C]}, \tag{9a}$$

$$k_{HC,A} = \frac{k_{31}}{[A^{-}]}. \tag{9b}$$

Similarly

$$HB^{+} + C \underset{k_{HC,B}}{\overset{k_{HB,C}}{\rightleftharpoons}} HC^{+} + B, \tag{10}$$

with

$$k_{HB,C} = \frac{k_{23}}{[B]}, \tag{11a}$$

$$k_{HC,B} = \frac{k_{32}}{[C]}. \tag{11b}$$

Here, $[A^{-}]$ is the concentration of anion, $[B]$, the concentration of water and $[C]$, that of acetone present in the solution at equilibrium.

Following (5) and using the above relations, the kinetic matrix in this case may thus be written as:

$$\frac{\mathrm{d}}{\mathrm{d}t}\begin{pmatrix} I_z - I_0 \\ S_z - S_0 \\ R_z - R_0 \end{pmatrix} = \begin{pmatrix} \begin{pmatrix} -\frac{1}{T_1} - 0{\cdot}2k_{21} \\ -0{\cdot}2k_{31} \end{pmatrix} & k_{21} & k_{31} \\ 0{\cdot}2k_{21} & \begin{pmatrix} -\frac{1}{T_1} - k_{21} \\ -k_{23} \end{pmatrix} & k_{23} \\ 0{\cdot}2k_{31} & k_{23} & \begin{pmatrix} -\frac{1}{T_1} - k_{23} \\ -k_{31} \end{pmatrix} \end{pmatrix} \begin{pmatrix} I_z - I_0 \\ S_z - S_0 \\ R_z - R_0 \end{pmatrix} \tag{12}$$

Further, for the proton exchange dynamics in superacid media,[37] the experimental first order rate coefficients k_{12} and k_{13} (7a and 9a) equal the inverse of the mean residence time of the proton on HA (site 1), while the first order rate coefficients k_{21} and k_{23} (7b and 11a) equal the inverse of the mean residence time of proton on HB^{+} (site 2) and the first order rate coefficients k_{31} and k_{32} (9b and 11b) correspond to the mean residence time of proton on HC^{+} (site 3), which are obtainable from NMR measurements. For the acid–base reaction given in (6) and (8), the following relations hold good at equilibrium:

$$K^{12} = \frac{k_{HA,B}}{k_{HB,A}} = \frac{[HB^+][A^-]}{[HA][B]}, \quad (13)$$

$$K^{13} = \frac{k_{HA,C}}{k_{HC,A}} = \frac{[HC^+][A^-]}{[HA][C]}. \quad (14)$$

Following the arguments of Gold *et al*[37] in the above equations the values of $k_{HA,B}$, $k_{HA,C}$ are assumed to be same for the solute bases *B* and *C* since the value of this constant must be large and close to the limit set by the rate of encounters.[37] Further, the value of $[A^-]/[HA]$ is known from the stoichiometric composition of the solution. This follows because $[A^-]$ must very closely approximate the sum of the initial concentrations ($[B]_0$, $[C]_0$) of the added bases *B* and *C* if the bases are almost completely converted into their conjugate acids. The formation of A^- is accompanied by a corresponding reduction of the concentration of HA. Furthermore, this implies that at equilibrium $[HB^+]$ must be essentially equal to $[B]_0$ while $[HC^+]$ must be essentially equal to $[C]_0$. The equilibrium constants K^{12} and K^{13} are then essentially independent of the concentration of the added bases under the condition of complete protonation of the bases – and depend only on the chemical composition of the solvent acid (in the present instance the stoichiometric proportion of fluorosulphonic acid and antimony pentafluoride).[37] Considering the ratio of the equilibrium constants, one may therefore write:

$$\frac{k_{HC,A}}{k_{HB,A}} = \frac{[HB^+]}{[HC^+]}. \quad (15)$$

Since the equilibrium concentrations of the two conjugate acids are equal as measured from the NMR intensities, i.e. $[HB^+] = [HC^+]$, it follows that:

$$k_{HB,A} = k_{HC,A}. \quad (16)$$

Equation (16) implies that the second order deprotonation rates of the two bases are equal under the condition of complete protonation of the two bases. This in turn results in equalization of the two first order rate constants, viz. k_{21}, k_{31}. Hence it may be concluded that only three unknown parameters, viz. T_1, $k_{21} = k_{31} = k$, k_{23} are to be determined from the kinetic equation given in (12) which is re-written as follows:

$$\frac{\mathrm{d}}{\mathrm{d}t}\begin{pmatrix} I_z - I_0 \\ S_z - S_0 \\ R_z - R_0 \end{pmatrix} = \begin{pmatrix} -\frac{1}{T_1} - 0{\cdot}4k & k & k \\ 0{\cdot}2k & -\frac{1}{T_1} - k - k_{23} & k_{23} \\ 0{\cdot}2k & k_{23} & -\frac{1}{T_1} - k_{23} - k \end{pmatrix} \begin{pmatrix} I_z - I_0 \\ S_z - S_0 \\ R_z - R_0 \end{pmatrix}. \quad (17)$$

The above differential equation may be solved for any arbitrary initial condition with the help of Mathematica, employing the actual population ratios of the three components.

The solution of (17) has been obtained by employing two different initial conditions with the help of Mathematica 5.1. To maintain compact notation, the mixing time τ_m is represented by *t* in all the following equations.

(i) $I_z(0) = -I_0$; $S_z(0) = -S_0$; $R_z(0) = -R_0$: A double cosine modulated pulse followed by a hard $\pi/2$ pulse results in this initial state. The corresponding solution is given in (18) in terms of the 'sum' magnetization that has a mono-exponential dependence on T_1 alone.

$$I_z + S_z + R_z = (I_0 + S_0 + R_0)\left[1 - 2\exp\left(-\frac{t}{T_1}\right)\right]. \quad (18)$$

(ii) $I_z(0) = I_0$; $S_z(0) = S_0$; $R_z(0) = R_0$: a cosine–sine modulated pulse followed by a hard $\pi/2$ pulse results in this initial condition where only the protonated acetone peak (site 3) is inverted. The analytical solutions (19, 20 and 21) for each of the three magnetization components now reveal the other two kinetic parameters, viz. *k* and k_{23}.

$$I_z = I_0 + \frac{2R_0 b}{p}\left[\exp\left(-\frac{lt}{2}\right) - \exp\left(-\frac{mt}{2}\right)\right] \quad (19)$$

$$S_z = S_0 + R_0 \exp[-(c+e)t] - \frac{R_0}{2p}\left[n\exp\left(-\frac{lt}{2}\right) + q\exp\left(-\frac{mt}{2}\right)\right], \quad (20)$$

$$R_z = R_0 - R_0 \exp[-(c+e)t] - \frac{R_0}{2p}\left[n\exp\left(-\frac{lt}{2}\right) + q\exp\left(-\frac{mt}{2}\right)\right], \quad (21)$$

Here

$$l = a + c - e + p; \quad m = a + c - e - p;$$
$$n = -a + c - e + p; \; q = a - c + e + p, \quad (22)$$

$$a = \frac{1}{T_1} + 0{\cdot}4k; \quad c = \frac{1}{T_1} + k + k_{23}; \; b = k; \; d = 0{\cdot}2k, \quad (23)$$

$$e = k_{23}; \; p = \sqrt{(a - c + e)^2 + 8bd}\,. \quad (24)$$

These solutions may be employed as fitting equations in order to derive the rate constants from the experimental data.

4. Results and discussion

Single pulse experiments are performed with a cosine modulated shaped pulse. The resulting line intensities after application of the cosine modulated Gaussian pulse follows a Gaussian profile as a function of frequency. This is in keeping with the fact that in the linear response regime the Fourier transform of the time domain pulse envelope is an excellent approximation to the excitation profile, barring relaxation effects.

The amplitude of the magnetization resulting after the cosine modulated Gaussian pulse for two simultaneously excited chemical sites has been plotted in arbitrary units (a.u.) against the frequency offset of the shaped pulse carrier in figure 4. It shows an expected Gaussian profile. In this case the shaped pulse carrier has been varied keeping the modulation frequency constant. The figure caption gives other relevant details of the experimental set-up. In a similar experiment modulation frequency of the cosine modulated Gaussian pulse has also been stepped up keeping the carrier frequency of the shaped pulse constant at the average of the two lines to be excited and one observes the expected Gaussian profile once again.

Figure 5 shows the spectra resulting after application of double cosine and cosine–sine modulated excitation pulses. The shaped pulse carrier frequency has been placed at the middle of the two lowest field peaks, viz. protonated acetone peak and the acid peak. Here pulse duration of 10 ms has been employed. A point to be noted here is that in case of exchange studies the choice of pulse duration is also governed by the required selectivity besides the

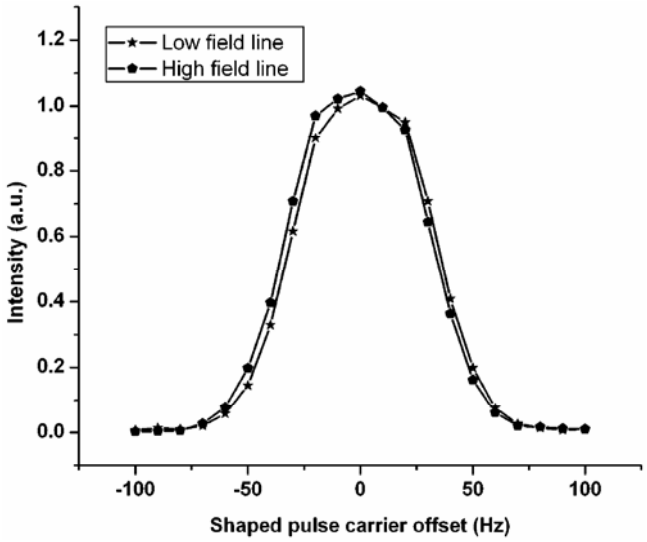

Figure 4. Experimental excitation profile obtained with the cosine modulated Gaussian pulse of duration 40 ms and modulation frequency of 100 Hz. The shaped pulse carrier frequency has been moved in 10 Hz steps from one chemical site to the other. The maximum amplitude corresponds to the positioning of the carrier at the average of the two frequencies excited. The resulting phase remains constant within ± 5% as a function of frequency offset.

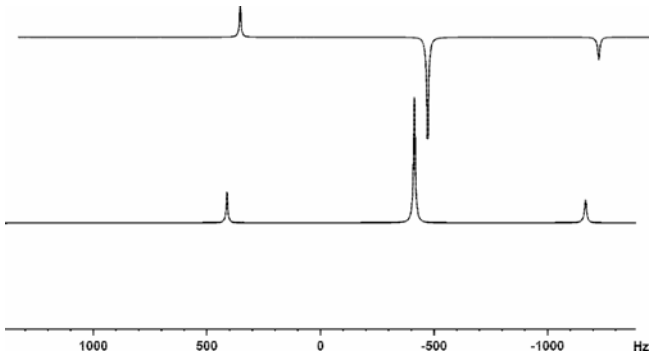

Figure 5. Spectra resulting after multi-site selective shaped pulse excitation; bottom trace: double cosine modulation resulting in simultaneous excitation of all the three peaks with same phase relations. The shaped pulse carrier frequency is placed at the average of the two lowest field signals, viz. the acid peak and the acetone peak; top trace: cosine–sine modulation resulting in simultaneous excitation of all the three sites with inversion of acid and water peaks.

anticipated k value at a particular temperature. Alternative shapes, e.g. sinc can be employed with shorter duration than a Gaussian to achieve a given selectivity.

Insertion of a double cosine modulated shaped pulse in the exchange sequence results in inversion of all the three sites whereas insertion of a cosine–sine modulated shaped pulse in the exchange sequence results in inversion of acetone peak alone. Figure 6 shows the stack plot at $T = 298$ K for the cosine–sine modulated inversion experiment as a function of τ_m. The un-inverted peaks in the case of the cosine–sine modulated experiment, viz. the acid and the water peak show the characteristic dip[49,50] in their intensity profiles whereas the protonated acetone peak exhibits the typical inversion recovery behaviour.

Using the fitting equations given in (18) and (21), the experimental data for the double cosine and the cosine–sine modulated experiments have been fitted to determine all the relevant kinetic parameters, viz. the spin-lattice relaxation time (T_1), the deprotonation rate constants for the two bases ($k_{21} = k_{31} = k$), as well as the proton exchange rate constant between water and acetone (k_{23}). Figure 7a shows the plot of experimental signal intensities vs mixing time corresponding to the 'sum' magnetization obtained from the double cosine modulated inversion experiment at $T = 298$ K, while figure 7b shows the plot of experimental signal intensities of the protonated acetone peak against mixing time at $T = 298$ K. In this case since the deprotonation rate constants for the two bases are equal ($k_{21} = k_{31} = k$), inversion of the acetone peak alone is sufficient to unravel all the exchange rate constants. The kinetic parameters thus obtained are given for nine different temperatures in table 3. The activation parameters corresponding to the deprotonation process are given in table 4 and are in good agreement with the literature values.[51]

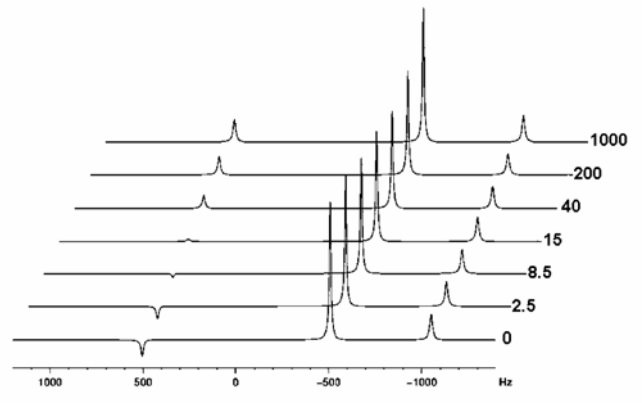

Figure 6. Stack plot of the cosine-sine modulated inversion experiment as a function of mixing time (τ_m) at $T = 298$ K. The respective τ_ms are given next to each spectrum in units of ms.

5. Conclusion

The present 1D exchange pulse sequence involves amplitude modulated shaped pulses; double modulation of the shaped pulse envelope has been exploited. Singly modulated shaped pulses may be employed, on the other hand, to study two-site exchange processes. Incorporation of such a modulated shaped pulse enables the creation of various

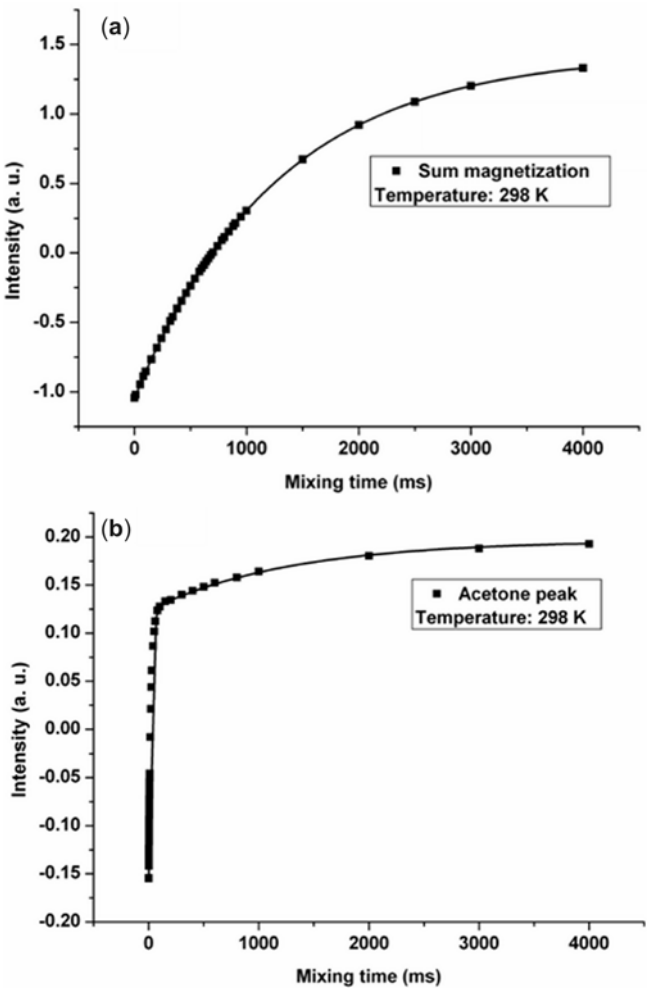

Figure 7. (**a**) Plot of 'sum' magnetization against τ_m at $T = 298$ K resulting from the double cosine modulated inversion recovery sequence; (**b**) plot of signal intensities of the acetone peak against τ_m at $T = 298$ K resulting from the cosine–sine modulated inversion recovery sequence.

Table 3. Kinetic parameters obtained for the proton exchange dynamics in magic acid solution modelled as three-site exchange process.

	Kinetic parameters		
Temperature T (K)	R_1 (s^{-1})	$K_{21} = k_{31}$ (s^{-1})	k_{23} (s^{-1})
233	2·74 ± 0·01	1·04 ± 0·01	0·36 ± 0·005
238	2·46 ± 0·04	1·65 ± 0·2	0·42 ± 0·02
243	2·23 ± 0·006	2·27 ± 0·14	0·66 ± 0·01
248	2·02 ± 0·002	3·88 ± 0·31	0·71 ± 0·02
253	1·85 ± 0·003	5·84 ± 0·42	1·08 ± 0·004
263	1·48 ± 0·002	12·88 ± 0·13	2·23 ± 0·03
273	1·21 ± 0·002	20·00 ± 1·34	3·32 ± 0·09
283	1·02 ± 0·004	30·65 ± 1·38	4·40 ± 0·06
298	0·78 ± 0·001	70·05 ± 0·31	6·17 ± 0·08

Table 4. Activation parameters obtained for the deprotonation process in magic acid solution.

Arrhenius parameters		Eyring parameters	
Activation energy E_a (kJ mol^{-1})	Frequency factor A (s^{-1})	Enthalpy of activation ΔH^* (kJ mol^{-1})	Entropy of activation ΔS^* (J mol^{-1} K^{-1})
37·33 ± 1·16	(2·62 ± 0·08) × 10^8	35·17 ± 1·66	−90·89 ± 4·48

initial states of the exchanging sites, avoids off-resonance effects, and ensures uniform pulse non-idealities for all exchanging sites. The 1D method described, permits a clear definition of the exchange time window; it also enables genuinely accurate measurements of the kinetic as well as activation parameters, since this fast experiment may be readily carried out – with standard hardware and software – at a large number of mixing times and at different temperatures, in a modest total experiment time.

One may employ the proposed pulse sequence even for closely spaced frequencies. The proposed pulse sequence has been successfully implemented to study amide rotation in dimethylacetamide by ^{1}H NMR (not reported) – this system exhibits only 0·4 ppm frequency separation between the two exchanging sites. Clearly on modern NMR machines that operate at 400 MHz and higher our simple modulated Gaussian or sinc pulses turn out to be efficient even for line spacing substantially less than a ppm. There are, of course, limits to improving selectivity by employing long shaped pulses, bearing in mind the constraint imposed by the exchange rate constant.

Analytical solutions for the kinetic parameters for a three-site exchange, which are valid under the conditions of the present study, have also been given.

Acknowledgements

The author gratefully acknowledges Prof. N Chandrakumar for his valuable suggestions during the experimental work and critical comments and corrections for the manuscript. The author thank Council of Scientific and Industrial Research (CSIR), India for the grant of a Senior Research Fellowship and a Spectrometer grant to the Department of Chemistry from Department of Science and Technology (DST), India.

References

1. Gutowsky H S and Saika A 1953 *J. Chem. Phys.* **21** 1688
2. Jackmann L M and Cotton F A (eds) 1975 *Dynamic NMR spectroscopy* (New York: Academic Press)
3. Forsén S and Hoffman R A 1963 *J. Chem. Phys.* **39** 2892
4. Forsén S and Hoffman R A 1964 *J. Chem. Phys.* **40** 1189
5. Inglefield P T, Krakower E, Reevs L W and Stewart R 1968 *Mol. Phys.* **15** 65
6. Dahlquist W, Longmuir K J and DuVernet R B 1975 *J. Magn. Reson.* **17** 406
7. Campbell D, Dobson C M and Ratcliffe R G 1977 *J. Magn. Reson.* **27** 455
8. Gutowsky S, Vold R L and Wells E J 1965 *J. Chem. Phys.* **43** 4107

9. Muhandiram D R and McClung R E D 1987 *J. Magn. Reson.* **71** 187
10. Levy G C and Nelson G 1972 *J. Am. Chem. Soc.* **94** 4897
11. Spencer R G S 2000 *J. Magn. Reson.* **142** 120
12. Jeener J, Meier B H, Bachmann P and Ernst R R 1979 *J. Chem. Phys.* **71** 4546
13. Macura S and Ernst R R 1982 *J. Magn. Reson.* **46** 269
14. Perrin C L 1989 *J. Magn. Reson.* **82** 619
15. Abel E W, Coston T P J, Orrell K G, Šik V and Stephenson D 1986 *J. Magn. Reson.* **70** 34
16. Yarnykh V L and Ustynyuk Y A 1993 *J. Magn. Reson.* **A102** 131
17. Bremer J 1984 *J. Am. Chem. Soc.* **106** 4691
18. Campbell D, Dobson C M, Ratcliffe R G and Williams R J P 1978 *J. Magn. Reson.* **29** 397
19. Rabinovitz M and Pines A 1969 *J. Am. Chem. Soc.* **91** 1585
20. Mann B E 1976 *J. Magn. Reson.* **21** 17
21. Mann B E 1977 *J. Magn. Reson.* **25** 91
22. Grassi M, Mann B E, Pickup B T and Spencer C M 1986 *J. Magn. Reson.* **69** 92
23. McClung R E D and Aarts G H M 1995 *J. Magn. Reson.* **A115** 145
24. Bain A D and Cramer J A 1993 *J. Magn. Reson.* **A103** 217
25. Bain A D and Cramer J A 1996 *J. Magn. Reson.* **A118** 21
26. Cavanagh J, Fairbrother W J, Palmer A G and Skelton N J 1996 *Protein NMR spectroscopy. Principles and practice* (San Diego, CA: Academic Press)
27. Zhou J and van Ziji P C 2006 *Prog. Nucl. Magn. Reson. Spectroc.* **48** 109
28. Galban J and Spencer R G 2007 *Magn. Reson. Med.* **58** 8
29. Lucchini V, Borsato G, Canovese L, Santo C, Visentin F and Zambon A 2009 *Inorg. Chim. Acta* **362** 2715
30. Hirose K, Ishibashi K, Shiba Y, Doi Y and Tobe Y 2008 *Chem. Eur. J.* **14** 5803
31. Bodenhausen G, Zwahlen C, Vincent S J F and Schwager M 1996 *Chem. Eur. J.* **2** 45
32. Shapira B and Frydman L 2003 *J. Magn. Reson.* **165** 320
33. Perrin C L and Engler R E 1996 *J. Magn. Reson.* **A123** 188
34. Bain A D, Bell R A, Fletcher D A, Hazendonk P, Maharajh R A, Rigby S and Valliant J F 1999 *J. Chem. Soc., Perkin Trans. II* **144** 7
35. Heaton B T, Jacob C, Podkorytov I S and Tunik S P 2006 *Inorg. Chim. Acta* **359** 3557
36. Gold V, Laali K, Morris K P and Zdunek L Z 1981 *J. Chem. Soc. Chem. Comm.* **769**
37. Gold V, Laali K, Morris K P and Zdunek, L Z 1985 *J. Chem. Soc., Perkin Trans. II* **859**
38. Bauer C, Freeman R, Frenkiel T, Keeler J and Shaka A J 1984 *J. Magn. Reson.* **58** 442
39. Hadamard J 1893 *Bull. Sci. Math.* **17** 240
40. Olah G A and Schlosberg R H 1968 *J. Am. Chem. Soc.* **90** 2726
41. Olah G A 2005 *J. Org. Chem.* **70** 2413
42. McConnell H M 1958 *J. Chem. Phys.* **28** 430
43. Bain A D and Cramer J A 1993 *J. Phys. Chem.* **97** 2884
44. Steigel A 1978 *NMR Basic principles and progress* (eds) P Diehl, E Fluck and R Kosfeld (Heidelberg: Springer-Verlag: Berlin) p. 15
45. Perrin C L and Gipe R K 1984 *J. Am. Chem. Soc.* **106** 4036
46. Perrin C L and Johnston E R 1979 *J. Magn. Reson.* **33** 619
47. Ugurbil K 1985 *J. Magn. Reson.* **64** 207
48. Ernst R R, Bodenhausen G and Wokaun W 1987 *Principles of nuclear magnetic resonance in one and two dimensions* (Oxford: Oxford University Press)
49. Bain A D 2003 *Prog. Nucl. Magn. Reson.* **43** 63
50. Bain A D 2008 *Ann. Rep. NMR Spectroc.* **63** 23
51. Gold V, Laali K, Morris K P and Zdunek L Z 1985 *J. Chem. Soc. Perkin Trans. II* 865